

Finite element based level set method with various reinitializations for viscous incompressible two-phase flows

Norikazu Yamaguchi

Faculty of Human Development, University of Toyama
3190 Gofuku, Toyama-shi, Toyama 930-8555, Japan

Abstract. The main objective of the present paper is numerical computation of viscous incompressible two-phase flows by finite element based level set method. A numerical result concerning quantitative benchmark problem proposed by Hysing *et al.* [11] is reported.

1. Introduction

In this paper, we are concerned with numerical simulation of two-dimensional viscous incompressible and immiscible two-phase flows by finite element based level set method.

The motion of viscous incompressible and immiscible two-phase flows is mathematically formulated as a free boundary value problem of the Navier-Stokes equations. In free boundary value problems of the Navier-Stokes equations, unknown variables are not only velocity and pressure but also the location of interface between two fluids. We are particularly interested in deformation of the interface and flow near the interface. Thus, numerical computation is one of the reasonable ways to observe them, because numerical computation enables us to see the development process of the motion and deformation.

Viscous incompressible two-phase flows include various interesting phenomena in fluid dynamics, e.g., rising bubble, droplet impact and dam breaking phenomena. Since there are a lot of literature concerning rising bubble problem in two space dimension, we also consider rising bubble problem in 2D (however we do not rely on any specialties of 2D for discretization of the problem). In particular, a numerical result concerning quantitative benchmark problem proposed by Hysing *et al.* [11] is reported.

The present paper is a part of joint work with N. Hamamuki (Hokkaido University) and K. Ohmori (University of Toyama). Details of our results will be published in a forthcoming paper.

1.1. Governing equations

First of all, let us give a governing equations of the incompressible two-phase flows.

Let $\Omega \subset \mathbb{R}^2$ be a bounded domain with boundary $\partial\Omega$. Ω is container of fluids and is assumed to be divided into two parts by interface $\Gamma(t)$, that is, $\Omega = \Omega_1(t) \cup \Gamma(t) \cup \Omega_2(t)$. Here and in what follows, $\Omega_j(t)$ is filled with fluid j ($j = 1, 2$) and fluid 1 and fluid 2 are immiscible, that is, $\Omega_1(t) \cap \Omega_2(t) = \emptyset$. Let ρ_j and ν_j be density and viscosity of

fluid j ($j = 1, 2$), respectively. Throughout the present paper, we assume that ρ_j and ν_j are constants ($j = 1, 2$).

The motion of fluids in Ω is governed by the Navier-Stokes equations.

$$\rho(\partial_t \mathbf{u} + \mathbf{u} \cdot \nabla \mathbf{u}) = \operatorname{div}(2\nu \mathbb{D}(\mathbf{u}) - p\mathbb{I}) + \mathbf{F}, \quad x \in \Omega, t > 0, \quad (1.1a)$$

$$\operatorname{div} \mathbf{u} = 0, \quad x \in \Omega, t > 0. \quad (1.1b)$$

The first equation (1.1a) is balance of momentum and second one (1.1b) is equation of continuity. Here $\mathbf{u} = (u_1(t, x), u_2(t, x))$ and $p = p(t, x)$ are velocity and pressure, respectively. They are unknown functions. $\rho = \rho(t, x)$ and $\nu = \nu(t, x)$ are density and viscosity which are given by

$$(\rho, \nu) = \begin{cases} (\rho_1, \nu_1), & x \in \Omega_1(t), \\ (\rho_2, \nu_2), & x \in \Omega_2(t). \end{cases} \quad (1.1c)$$

For the density of fluids, we assume that $\rho_1 > \rho_2$, that is, fluid 1 is heavier than fluid 2 (for example, fluid 1 is water and fluid 2 is oil or air). $\mathbb{D}(\mathbf{u}) = ((\partial_j u_i + \partial_i u_j)/2)_{1 \leq i, j \leq 2}$ is the deformation tensor and $\mathbb{I} = (\delta_{ij})_{1 \leq i, j \leq 2}$ is the 2×2 unit matrix. $2\nu \mathbb{D}(\mathbf{u}) - p\mathbb{I}$ is the Cauchy stress tensor associated with flow. \mathbf{F} denotes the body force acting on fluid. In what follows, we suppose that \mathbf{F} is gravitational force given by

$$\mathbf{F} = \mathbf{f}_{\text{gravity}} = (0, -\rho g), \quad (1.1d)$$

where g is a positive constant which indicates gravitational acceleration.

In addition to \mathbf{u} and p , location of interface $\Gamma(t)$ is also unknown in two-phase flows. We need additional equation on the interface $\Gamma(t)$. On the interface $\Gamma(t)$, the surface tension is taken into account. Thus, the interface conditions on $\Gamma(t)$ are as follows.

$$[\mathbf{u}]|_{\Gamma(t)} = \mathbf{0}, \quad [2\nu \mathbb{D}(\mathbf{u}) - p\mathbb{I}]|_{\Gamma(t)} \cdot \mathbf{n}_{\Gamma(t)} = \sigma \kappa \mathbf{n}_{\Gamma(t)}. \quad (1.1e)$$

Here $\sigma > 0$ denotes surface tension constant, $\kappa = \kappa(t, \mathbf{x})$ is the curvature of the interface $\Gamma(t)$, and $\mathbf{n}_{\Gamma(t)}$ is unit normal at the interface $\Gamma(t)$ pointing into $\Omega_1(t)$. Square bracket denotes jump of quantity “ \bullet ”:

$$[\bullet]_{\Gamma(t)} = \bullet|_{\Omega_1 \cap \Gamma(t)} - \bullet|_{\Omega_2 \cap \Gamma(t)}.$$

The interface condition (1.1e) implies that the velocity continuously across the interface $\Gamma(t)$ and surface tension balances the jump of normal stress.

To observe motion of fluids in Ω by means of numerical computation, we will solve initial boundary value problem of (1.1) with initial velocity $\mathbf{u}(t, \mathbf{0}) = \mathbf{u}_0$, initial interface $\Gamma(0) \subset \Omega$ and some boundary condition for (\mathbf{u}, p) on $\partial\Omega$.

1.2. Related works and aim of the paper

As was mentioned, we consider only rising bubble problem. Since rising bubble is a typical phenomena of interfacial flows, there are much related works. Sussman, Smereka & Osher [23] studied rising bubble problem in 2D by finite difference based level set method. The level set method introduced in Osher & Sethian [17] is one of the standard ways to capture the interface $\Gamma(t)$ in numerical computation of interfacial flows. The basic idea of our method is due to [23].

Concerning rising bubble problem, there are also a lot of related works by finite element method, e.g., Gross, Reichelt & Reusken [6], Tabata [24], Tornberg & Engquist [26], Gross & Reusken [7] and references therein. Concerning rising bubble problem by finite element method, Hysing *et al.* [11] proposed a quantitative benchmark problem (see also Doyeux *et al.* [5]). Our aim of the present paper is contribute the benchmark problem proposed by Hysing *et al.* [11].

As will be seen in Section 2, interface $\Gamma(t)$ can be tracked by transport equation of the level set function (interface is characterized by zero level set of level set function). The level set function is required to have signed distance function property. However, transport equation does not conserve such a property. Therefore we have to maintain such a property in numerical computation. The procedure of signed distance function maintenance is called reinitialization. There are various ways of reinitialization, e.g., method based on partial differential equations and fast marching method (see e.g., [7]).

We adopt reinitialization based on partial differential equations. In [23], reinitialization based on first order hyperbolic equation was introduced. Later on [23], Sussman & Fatemi [22] proposed a modified version of [23] (see also [8]). Recently, new reinitialization procedures are proposed by Liu *et al.* [12] and Basting & Kuzmin [1]. The method of [1] is based on nonlinear elliptic partial differential equation. Therefore it is easy to implement the method of [1] in terms of finite element method. In particular, the method of [1] seems to be good one from a point view of computational cost. We use classical reinitialization [23, 22] and reinitialization due to Basting & Kuzmin [1] in our numerical computation (only the latter case is reported. The former case will be reported in separate paper).

1.3. Organization of the paper

This paper is organized as follows. In Section 2 the level set method is introduced. By using the level set method we reformulate the free boundary value problem of (1.1) to be suitable form for numerical computation. Discretization of reformulated problem is also given in Section 2. In Section 3 reinitialization of the level set function is discussed. Two reinitializations based on partial differential equations are introduced. We show our numerical result in Section 4. We use FreeFem++ for our computation.

2. Level set method and discretization

The level set method introduced by Osher & Sethian [17] is one of the convenient ways to capture the interface $\Gamma(t)$ in two-phase flows. In this section, we shall give a reformulated problem of (1.1) by the level set method and give a discrete approximation of resultant problem.

2.1. Level set method

To capture the interface $\Gamma(t)$ in numerical computation, we are due to the level set method introduced by Osher & Sethian [17]. First of all, let us introduce the level set function. Let $\phi = \phi(t, \mathbf{x})$ be a continuous scalar function defined on entire domain Ω and $t > 0$, whose value is positive for $\mathbf{x} \in \Omega_1(t)$, negative for $\mathbf{x} \in \Omega_2(t)$ and zero for $\mathbf{x} \in \Gamma(t)$. Then we call function ϕ the level set function.

A suitable choice is to take ϕ equal to signed distance function to the interface $\Gamma(t)$.

$$\phi(t, \mathbf{x}) = \begin{cases} \text{dist}(\mathbf{x}, \Gamma(t)), & \mathbf{x} \in \Omega_1(t), \\ 0, & \mathbf{x} \in \Gamma(t), \\ -\text{dist}(\mathbf{x}, \Gamma(t)), & \mathbf{x} \in \Omega_2(t). \end{cases} \quad (2.1)$$

Here dist denotes the distance function: $\text{dist}(\mathbf{x}, \Gamma) = \min_{\mathbf{y} \in \Gamma} |\mathbf{x} - \mathbf{y}|$. Since ϕ is signed distance function, $|\nabla\phi| = 1$ (a.e.) must be satisfied. From (2.1), it is clear that zero level set of ϕ characterizes the interface $\Gamma(t)$.

$$\Gamma(t) = \{\mathbf{x} \in \Omega \mid \phi(t, \mathbf{x}) = 0\}. \quad (2.2)$$

When we choose $\phi_0 = \phi_0(\mathbf{x})$ in such a way that ϕ_0 is signed distance function to the initial interface $\Gamma(0)$, the level set function ϕ is transported by the following transport equation:

$$\frac{\partial\phi}{\partial t} + \mathbf{u} \cdot \nabla\phi = 0, \quad t > 0, \quad \mathbf{x} \in \Omega, \quad (2.3a)$$

$$\phi(0, \mathbf{x}) = \phi_0(\mathbf{x}), \quad \mathbf{x} \in \Omega. \quad (2.3b)$$

Since the interface $\Gamma(t)$ is represented as (2.2), it is enough to solve the above transport equation (2.3) (numerically) and investigate the zero level set of ϕ .

Next we consider a reformulation of the Navier-Stokes equations (1.1a). The level set function ϕ enables us to reformulate $\Omega_j(t), \Gamma(t)$ and (ρ, ν) as convenient representation for our purpose. By using the level set function ϕ , Ω and (ρ, ν) are rewritten as follows.

$$\Omega = \begin{cases} \Omega_1(t), & \phi > 0, \\ \Gamma(t), & \phi = 0, \\ \Omega_2(t), & \phi < 0; \end{cases} \quad (\rho, \nu) = \begin{cases} (\rho_1, \nu_1), & \phi > 0, \\ (\rho_2, \nu_2), & \phi < 0. \end{cases} \quad (2.4)$$

For later purposes, we now introduce the Heviside function $H(\phi)$.

$$H(\phi) = \begin{cases} 1, & \phi \geq 0, \\ 0, & \phi < 0. \end{cases} \quad (2.5)$$

By using $H(\phi)$, ρ and ν in (2.4) are rewritten as follows.

$$\rho = \rho(\phi) = \rho_1 H(\phi) + \rho_2 (1 - H(\phi)) = \rho_2 + (\rho_1 - \rho_2) H(\phi), \quad (2.6)$$

$$\nu = \nu(\phi) = \nu_1 H(\phi) + \nu_2 (1 - H(\phi)) = \nu_2 + (\nu_1 - \nu_2) H(\phi). \quad (2.7)$$

Next we shall give a level set formulation of the surface tension (1.1e). By using level set function ϕ , the surface tension force is converted into a volume force of the form

$$\mathbf{f}_{\text{ST}} = \sigma \kappa \mathbf{n}_{\Gamma(t)} \delta(\phi). \quad (2.8)$$

Here and in what follows, $\delta(\phi)$ denotes Dirac's delta function whose support is the zero level set of ϕ . Furthermore, normal vector $\mathbf{n}_{\Gamma(t)}$ and curvature κ are also given by

$$\mathbf{n}_{\Gamma(t)} = \frac{\nabla\phi}{|\nabla\phi|} \Big|_{\phi=0}, \quad (2.9)$$

$$\kappa(t) = -\text{div} \mathbf{n}_{\Gamma(t)} = -\text{div} \frac{\nabla\phi}{|\nabla\phi|} \Big|_{\phi=0}. \quad (2.10)$$

Summing up the above, the resultant problem is the following system of Navier-Stokes equations and transport equation.

$$\rho(\phi)(\partial_t \mathbf{u} + \mathbf{u} \cdot \nabla \mathbf{u}) = \operatorname{div}(2\nu(\phi)\mathbb{D}(\mathbf{u}) - p\mathbb{I}) + \mathbf{f}_{\text{ST}} + \mathbf{f}_{\text{gravity}}, \quad (2.11a)$$

$$\operatorname{div} \mathbf{u} = 0, \quad (2.11b)$$

$$\partial_t \phi + \mathbf{u} \cdot \nabla \phi = 0. \quad (2.11c)$$

By the level set function, our aim is reduced to solve initial boundary value problem of (2.11) with appropriate initial data $(\mathbf{u}, \phi)|_{t=0}$ and boundary conditions.

2.2. Discretization

In this subsection, we shall give a discretization for (2.11).

Approximation of $\delta_\varepsilon(\phi)$ and $H_\varepsilon(\phi)$. For numerical computation of (2.11), we need some approximations of $H(\phi)$ and $\delta(\phi)$ in terms of continuous functions defined over Ω . So, instead of $H(\phi)$ and $\delta(\phi)$, we use the following $H_\varepsilon(\phi)$ and $\delta_\varepsilon(\phi)$ with some $\varepsilon > 0$.

$$H(\phi) \approx H_\varepsilon(\phi) = \begin{cases} 1, & \phi \geq \varepsilon, \\ \frac{1}{2} + \frac{1}{2} \left(\frac{\phi}{\varepsilon} + \frac{1}{\pi} \sin \left(\frac{\pi\phi}{\varepsilon} \right) \right), & |\phi| < \varepsilon, \\ 0, & \phi \leq -\varepsilon \end{cases} \quad (2.12)$$

and

$$\delta(\phi) \approx \delta_\varepsilon(\phi) = \frac{d}{d\phi} H_\varepsilon(\phi) = \begin{cases} \frac{1}{2\varepsilon} \left(1 + \cos \left(\frac{\pi\phi}{\varepsilon} \right) \right), & |\phi| < \varepsilon, \\ 0, & |\phi| \geq \varepsilon. \end{cases} \quad (2.13)$$

Here $\varepsilon > 0$ denotes thickness of the numerical interface. Since ideal thickness of the interface is equal to zero, we would like to take $\varepsilon > 0$ as small as possible. However, we need to choose $\varepsilon > 0$ in such a way that $\varepsilon > h$, where h denotes the mesh size near the interface. A typical choice of ε is $\frac{3}{2}h$, where $h > 0$ indicates the mesh size near the $\Gamma(t)$. As will be seen in Section 4, we use adaptive mesh refinement (AMR). According to AMR, we can put a lot of mesh points near the interface. Hence, we can choose $\varepsilon > 0$ suitably small (see Figure 4.3).

Penalty method. One of the main difficulties of the Navier-Stokes equations is caused by pressure term p in (1.1a) and divergence free constraint (1.1b).

To relax difficulties arising from the pressure, some stabilization techniques are widely used in numerical computation of the Navier-Stokes equations. We here use the penalty method introduced by Temam [25]. Let $\alpha > 0$ be parameter of penalization. Then we shall replace the solenoidal condition (1.1b) by following one.

$$\operatorname{div} \mathbf{u} = -\alpha p. \quad (2.14)$$

It would be expected that $(\mathbf{u}^{(\alpha)}, p^{(\alpha)})$, which denotes solution of the Navier-Stokes equations with (2.14), tends to genuine solution (\mathbf{u}, p) as $\alpha \rightarrow +\infty$. Actually, such a limit is justified by Temam [25], Shen [20] and the author [27] for stationary and instationary problems.

In context of finite element method, (2.14) changes the variational structure of the Stokes equations (see, e.g., Pironneau [18]).

Characteristic method. For approximation of the convection terms in the Navier-Stokes equations (2.11a) and transport equation (2.3a), we are due to characteristic method (see e.g., Pironneau [18]).

Let $\mathbf{w} \in \mathbb{R}^m$ ($m \geq 2$) be given vector field. Then we consider material derivative of scalar function φ with vector \mathbf{w} .

$$\frac{D\varphi}{Dt} := \frac{\partial\varphi}{\partial t} + \mathbf{w} \cdot \nabla\varphi. \quad (2.15)$$

Suppose that vector field $\mathbf{X}(t) \in \mathbb{R}^m$ defined on $(0, T]$ solves the following ordinary differential equations.

$$\frac{d\mathbf{X}}{dt} = \mathbf{w}(t, \mathbf{X}(t)). \quad (2.16)$$

By chain rule, we see that

$$\frac{d\varphi}{dt}(t, \mathbf{X}(t)) = \frac{D\varphi}{Dt}. \quad (2.17)$$

Let $\tau > 0$ be time step size. Applying the backward Euler approximation to the left hand side of (2.17), we obtain

$$\frac{D\varphi}{Dt} = \frac{\varphi(t, \mathbf{X}(t)) - \varphi(t - \tau, \mathbf{X}(t - \tau))}{\tau} + O(\tau). \quad (2.18)$$

Set $t_n = n\tau$ ($n \in \mathbb{N} \cup \{0\}$). Let $\mathbf{x} \in \Omega \subset \mathbb{R}^m$ be arbitrary point and let us consider initial value problem of (2.16) with initial condition $\mathbf{X}(t_n) = \mathbf{x}$. Then the genuine solution of such an initial value problem at $t = t_{n-1}$ is given by $\mathbf{X}(t_{n-1}) = \mathbf{X}^n + O(\tau^2)$, where $\mathbf{X}^n = \mathbf{x} - \mathbf{w}(t_n, \mathbf{x})\tau$ is approximate solution of (2.16) with the aid of Euler method. By the above arguments and Taylor's theorem, we have

$$\frac{D\varphi}{Dt}(t_n, \mathbf{x}) = \frac{\varphi(t_n, \mathbf{x}) - \varphi(t_{n-1}, \mathbf{X}^n)}{\tau} + O(\tau). \quad (2.19)$$

(2.19) gives us a first order approximation of the material derivative (2.15). Second order approximation for convection-diffusion or Navier-Stokes equations is also found in Rui & Tabata [19], Notsu & Tabata [13] and Benítez & Bermúdez [2].

Semi-discretization in time. We are now in a position to give a semi-discretization in time for (2.11).

Let $(\mathbf{u}^n, p^n, \phi^n) = (\mathbf{u}^n(\mathbf{x}), p^n(\mathbf{x}), \phi^n(\mathbf{x}))$ be approximation of $(\mathbf{u}, p, \phi)|_{t=t_n}$ ($t_n = n\tau$). Applying the characteristic approximation and penalty method to (2.11), we have the following semi-discretization in time for (2.11).

$$\rho_\varepsilon(\phi^n) \frac{\mathbf{u}^{n+1} - \mathbf{u}^n \circ \mathbf{X}^n}{\tau} = \operatorname{div}(2\nu_\varepsilon(\phi^n)\mathbb{D}(\mathbf{u}^{n+1}) - p^{n+1}\mathbb{I}) + \mathbf{f}_{\text{ST}}^n + \mathbf{f}_{\text{gravity}}^n, \quad (2.20a)$$

$$\operatorname{div} \mathbf{u}^{n+1} + \alpha p^{n+1} = 0, \quad (2.20b)$$

$$\frac{\phi^{n+1} - \phi^n \circ \mathbf{X}^n}{\tau} = 0, \quad (2.20c)$$

where $\mathbf{X}^n = \mathbf{x} - \mathbf{u}^n\tau$ and

$$\begin{aligned} \rho_\varepsilon(\phi^n) &= \rho_2 + (\rho_1 - \rho_2)H_\varepsilon(\phi^n), \\ \nu_\varepsilon(\phi^n) &= \nu_2 + (\nu_1 - \nu_2)H_\varepsilon(\phi^n), \\ \mathbf{f}_{\text{ST}}^n &= \sigma \kappa_\varepsilon^n|_{\Gamma(t_n)} \delta_\varepsilon(\phi^n), \quad \mathbf{f}_{\text{gravity}}^n = (0, -\rho_\varepsilon(\phi^n)\mathbf{g}), \\ \mathbf{n}_\varepsilon^n|_{\Gamma(t_n)} &= \frac{\nabla\phi^n}{|\nabla\phi^n|^2 + \varepsilon^2}, \quad \kappa_\varepsilon^n = -\operatorname{div} \mathbf{n}_\varepsilon^n|_{\Gamma(t_n)}. \end{aligned}$$

Assume that triplet $(\mathbf{u}^n, p^n, \phi^n)$ is given in (2.20). Then the system of (2.20a) and (2.20b) is the Stokes type system concerning unknown variables $(\mathbf{u}^{n+1}, p^{n+1})$. Hence, standard techniques to solve the Stokes type system by finite element method (see .e.g, [3], [18]) can be applicable.

Full discretization. Finally we consider full discretization for (2.11). Let \mathbf{V}_h, Π_h and X_h be finite dimensional spaces so that $\mathbf{V}_h \subset H^1(\Omega)^2, \Pi_h \subset L^2_0(\Omega), X_h \subset L^2(\Omega)$. Here

$$L^2_0(\Omega) = \left\{ p \in L^2(\Omega) \mid \int_{\Omega} p \, dx = 0 \right\}.$$

For numerical stability, we choose $\mathbf{V}_h \times \Pi_h$ as P2-P1 finite element space (standard Hood-Taylor elements) and X_h as P1 finite element space.

Considering variational formulation of semi discretized problem (2.20) and its approximation, we arrive at full discretization of (2.11a) and (2.11b): Find $(\mathbf{u}_h^{n+1}, p_h^{n+1})$ so that

$$\begin{aligned} & \frac{1}{\tau} (\rho_{\varepsilon}(\phi_h^n) \mathbf{u}_h^{n+1}, \mathbf{v}_h) + (2\nu_{\varepsilon}(\phi_h^n) \mathbb{D}_h(\mathbf{u}_h^{n+1}), \mathbb{D}_h(\mathbf{v}_h)) \\ & - (p_h^{n+1}, \operatorname{div}_h \mathbf{v}_h) = \frac{1}{\tau} (\mathbf{u}_h^n \circ \mathbf{X}^n) + (\mathbf{F}(\phi_h^n), \mathbf{v}_h) + \text{b.d.t.}, \end{aligned} \quad (2.21a)$$

$$(\operatorname{div}_h \mathbf{u}_h^{n+1} + \alpha p_h^{n+1}, q_h) = 0, \quad (2.21b)$$

for any $\mathbf{v}_h \in \mathbf{V}_h$ and $q_h \in \Pi_h$. Here “b.d.t.” denotes terms arising from boundary and (\cdot, \cdot) denotes L^2 inner product. For the transport equation, we do not need to consider weak formulation. Hence by (2.20c), we have the following explicit formula.

$$\phi_h^{n+1} = \tau \phi_h^n \circ \mathbf{X}^n. \quad (2.21c)$$

Of course it is possible to consider weak formulation associated with (2.20c).

3. Reinitialization

Level set method is one of the suitable methods for numerical computation of interfacial problems. In two-phase flows, the level set $\phi = \phi(t, \mathbf{x})$ is driven by transport equation (2.3). As was stated before, ϕ must be a signed distance function (SDF), which satisfy the Eikonal equation $|\nabla \phi| = 1$ (a.e.). However, the transport equation (2.3) does not conserve such a property even if the initial data ϕ_0 has SDF property.

In numerical computation, ϕ_h^n may lose such an important property in numerical computation as n increases. As a consequence of this undesirable behavior, numerical result will be incorrect, if we do not use any maintenance for level set function.

The procedure for recovering SDF property is called *reinitialization* (or *redistancing*). There are several ways of reinitialization. In this paper, we consider two reinitialization procedures based on partial differential equations (PDEs). The first one is classical procedure proposed by Sussman, Smereka & Osher [23]. The first procedure is based on a first order hyperbolic PDE. The second one is recent development by Basting & Kuzmin [1]. The second procedure is based on a nonlinear elliptic PDE, which can be regarded as a stationary problem of diffusion/anti-diffusion equation.

3.1. Reinitialization with hyperbolic PDE

Sussman, Smereka & Osher [23] studied incompressible two-phase flows by finite difference based level set method. In [23], they introduced a reinitialization based on hyperbolic PDE and reported its effectiveness by some numerical computations.

The reinitialization based on hyperbolic PDE is summarized as follows. Suppose that $\phi = \phi(t, \mathbf{x})$ is a level set function, but it does not have SDF property ($|\nabla\phi| = 1$ (a.e.)). Obtaining some function ψ so that ψ has the same zero level set as ϕ and has SDF property is objective of reinitialization. Let $\psi = \psi(s, \mathbf{x}; t)$ be solution to the following initial value problem.

$$\frac{\partial\psi}{\partial s} = \text{sgn}(\phi)(1 - |\nabla\psi|), \quad s > 0, \mathbf{x} \in \mathbb{R}^2, \quad (3.1a)$$

$$\psi(0, \mathbf{x}; t) = \phi(t, \mathbf{x}), \quad \mathbf{x} \in \mathbb{R}^2. \quad (3.1b)$$

where $s \geq 0$ indicates pseudo-time. If ψ is stationary solution of (3.1a), then it would be expected that ψ has SDF property (if such a stationary solution is asymptotically stable). Hence for sufficiently large $s > 0$, one can use $\psi(s, \mathbf{x}; t)$ as reinitialized ϕ . Such a numerical solution can be obtained by pseudo time stepping.

Since (3.1a) is first order hyperbolic partial differential equation, we need some stabilization technique for stable numerical computation. Converting (3.1a) into convective form is one of suitable reformulations. Set $\mathbf{w} = \text{sgn}(\phi)\nabla\psi/|\nabla\psi|$. Then (3.1a) is rewritten as the following equation.

$$\frac{\partial\psi}{\partial s} + \mathbf{w} \cdot \nabla\psi = \text{sgn}(\phi), \quad \mathbf{w} = \text{sgn}(\phi) \frac{\nabla\psi}{|\nabla\psi|}. \quad (3.2)$$

Since (3.2) is a transport equation with source term, stabilization technique (e.g., characteristic method and upwind techniques) can be applied.

In numerical computation for initial value problem (3.2), we need appropriate approximation of the sign function $\text{sgn}(\phi)$. Typical ways of approximations are

$$\text{sgn}(\phi) \approx \text{sgn}_\varepsilon(\phi) = \frac{\phi}{\sqrt{\phi^2 + \varepsilon^2}} \quad \text{or} \quad \frac{\phi}{\sqrt{\phi^2 + \varepsilon^2|\nabla\phi|^2}} \quad (3.3)$$

with parameter $\varepsilon > 0$, which is a regularization parameter. The size of ε is suitably determined by h which indicates the mesh size near the interface. It should be noted that $\text{sgn}(\phi)$ and $\text{sgn}_\varepsilon(\phi)$ has the same sign. Hence the regularization (3.3) conserves zero level set of ϕ .

As far as the author knows, there are no rigorous justification that asymptotic profiles of (3.1) is signed distance function to the zero level set of ϕ . For such a problem, we have a mathematical result as follows.

Theorem 3.1. *Let $d(\mathbf{x})$ be signed distance function to the zero level set of ϕ , whose sign is the same as ϕ . Then there hold that the solution of (3.1) tends to $d(\mathbf{x})$ as $s \rightarrow \infty$ locally and uniformly in \mathbb{R}^2 .*

Theorem 3.1 is a mathematical justification of the reinitialization based on (3.1). Proof is carried out with theory of viscosity solution [4]. Details will be published in a separate paper.

3.2. Reinitialization with elliptic PDE

Recently Basting & Kuzmin [1] introduced a reinitialization based on energy minimizing principle. According to Basting & Kuzmin [1], we shall explain reinitialization with elliptic PDE.

In context of pure reinitialization, reinitialized level set function would be stationary solution to an energy minimizing gradient flow of the form

$$\frac{\partial \psi}{\partial s} + \frac{\partial E}{\partial \psi} = 0, \quad (3.4)$$

where $E(\psi)$ is a suitable energy functional and $\partial E/\partial \psi$ is the Euler-Lagrange form of the Gâteaux derivative. The least-squares solution to the Eikonal equation $|\nabla \psi| = 1$ is defined by

$$E(\psi) = \frac{1}{2} \int_{\Omega} (|\nabla \psi| - 1)^2 dx. \quad (3.5)$$

By using (3.5), (3.4) is reduced to the nonlinear parabolic equation

$$\frac{\partial \psi}{\partial s} - \operatorname{div} \left(\nabla \psi - \frac{\nabla \psi}{|\nabla \psi|} \right) = 0. \quad (3.6)$$

If $|\nabla \psi| > 1$, then (3.6) is diffusion. On the other hand if $|\nabla \psi| < 1$, then (3.6) is anti-diffusion. (3.6) provides us a reinitialization with parabolic PDE. If initial data is given by original level set function ϕ , which does not have SDF property. Then asymptotic profile of (3.6) would be reinitialized level set function.

To obtain reinitialized level set function by (3.2) or (3.6), we need pseudo-time stepping. Basting & Kuzmin [1] proposed a reinitialization based on penalized minimizing problem such that

$$\frac{\partial E}{\partial \psi} + \frac{\partial P}{\partial \psi} = 0, \quad P(\psi; \phi) = \frac{\beta}{2} \int_{\{\phi=0\}} \psi^2 d\sigma \quad (3.7)$$

where $\beta \gg 1$ is parameter of penalization. Since any displacement of the zero level set would increase the value of $P(\psi; \phi)$, the numerical solution will preserve the shape of zero level set of ϕ for large β .

Let ϕ be a level set function without SDF property. A variational formulation associated with (3.5) is given by

$$\left(\left(1 - \frac{1}{|\nabla \psi|} \right) \nabla \psi, \nabla \varphi \right)_{\Omega} + \beta \langle \psi, \varphi \rangle_{\{\phi=0\}} = 0, \quad (3.8)$$

for any $\varphi \in C^{\infty}(\Omega)$. Since (3.8) can be regarded as a weak formulation of a nonlinear elliptic PDE, one can easily compute numerical solution to (3.8) by finite element method. Of course (3.8) is nonlinear, we seek numerical solution to (3.8) by successive approximation as follows.

$$\psi^{(0)} = \phi, \quad (3.9a)$$

$$(\nabla \psi^{(n+1)}, \nabla \varphi) + \beta \langle \psi^{(n+1)}, \varphi \rangle_{\{\phi=0\}} = \left(\frac{\nabla \psi^{(n)}}{|\nabla \psi^{(n)}|}, \varphi \right), \quad n \geq 0. \quad (3.9b)$$

If $\psi^{(n)}$ is given, (3.9b) can be regarded as a weak formulation of Poisson type equation with penalty term. One can obtain numerical solution to (3.9b) by finite element method.

4. Numerical experiments

In this section, we shall report our numerical result.

4.1. Quantitative benchmark problem

As was mentioned in Section 1, Hysing *et al.* [11] introduced a *quantitative* benchmark problem of two dimensional rising bubble (precise settings of the benchmark problem will be shown). Since exact solution for rising bubble problem is not known, it seems to be worthwhile well to compare numerical solution with other numerical solutions by such a quantitative benchmark problem.

Hysing *et al.* [11] studied two test cases (Case 1 and Case 2) by quantitative comparison between three European research groups. Two groups are adopted finite element based level set method. Later on [11], Doyeux *et al.* [5] also tried the same benchmark problem by Feel++. We also try the quantitative benchmark problem.

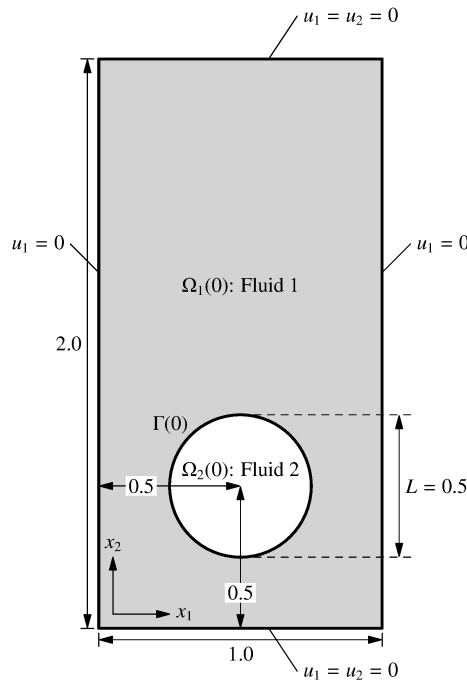


Figure 4.1: Initial state and boundary conditions

Initial state and boundary conditions. In the benchmark problem, the container of fluids is given by $\Omega = (0, 1) \times (0, 2)$. Initially bubble (=fluid 2) is completely surrounded by fluid 1 and shape of initial bubble is circle with radius $r_0 (= 0.25)$ centered at $(0.5, 0.5)$. To be precise, initial interface is given by

$$\Gamma(0) = \{(x_1, x_2) \mid (x_1 - 0.5)^2 + (x_2 - 0.5)^2 = r_0^2\}, \quad r_0 = 0.25. \quad (4.1)$$

For (4.1), initial level set function is signed distance function to $\Gamma(0)$, which is given by

$$\phi_0 = \sqrt{(x_1 - 0.5)^2 + (x_2 - 0.5)^2} - r_0^2. \quad (4.2)$$

Next we shall mention the boundary conditions. On the top/bottom walls of Ω , non-slip boundary condition $\mathbf{u} = \mathbf{0}$ is imposed and on the left/right walls of Ω , free slip

boundary condition:

$$\mathbf{u} \cdot \mathbf{n} = 0, \quad (\mathbb{D}(\mathbf{u})\mathbf{n}) - (\mathbf{n} \cdot \mathbb{D}(\mathbf{u})\mathbf{n}) = \mathbf{0}, \quad \mathbf{x} \in \partial\Omega_{\text{top/bottom}} \quad (4.3)$$

is imposed (the second condition is Neumann type boundary conditions for tangential component of the normal stress). Since the unit outer normal to left/right walls is $(\mp 1, 0)$, (4.3) is reduced to $u_1 = 0$.

Figure 4.1 is a image of initial configuration of the benchmark problem.

Physical constants. Two dimensionless numbers are used in rising bubble problem. Below, \mathcal{R} and \mathcal{E} denote the Reynolds number and Eötvös number (Bond number), respectively. \mathcal{R} and \mathcal{E} are defined as follows.

$$\mathcal{R} = \frac{\rho_1 V_g L}{\nu_1}, \quad \mathcal{E} = \frac{\rho_1 V_g^2 L}{\sigma}, \quad (4.4)$$

where $V_g = \sqrt{2gr_0}$ is the gravitational velocity, $L = 2r_0$ is characteristic length. The Eötvös number indicates the ratio of gravitational forces to surface tension. Table 4.1 lists the physical constants and dimensionless numbers which specify two test cases.

Table 4.1: Physical constants and dimensionless numbers

	ρ_1	ρ_2	ν_1	ν_2	g	σ	\mathcal{R}	\mathcal{E}
Case 1	1000	1	10	1	0.98	24.5	35	10
Case 2	1000	1	10	0.1	0.98	1.96	35	125

Roughly speaking, the surface tension is strong in Case 1 and weak in Case 2. Since the surface tension is strong in Case 1, we have to take temporal step size τ very small for numerical stability. Therefore we require much computational costs. However, strong surface tension force make shape of bubble stable. Actually, bubble is not splitted in our numerical computation. On the other hand, bubble would split, because of weak surface tension. In stability of the shape of bubble, Case 2 is more severe than Case 1.

In this paper, we shall try only Case 2. Our numerical result concerning Case 1 will be reported in a separated paper.

Benchmark values. In benchmark problem of Hysing *et al.* [11], some benchmark quantities are used.

Center of mass. To track the translation of bubble, it is common to use the center of mass defined as follows.

$$\mathbf{X}_c(t) = (X_{c,1}(t), X_{c,2}(t)), \quad X_{c,j}(t) = \frac{1}{|\Omega_2(t)|} \int_{\Omega_2(t)} x_j d\mathbf{x} \quad (j = 1, 2). \quad (4.5)$$

$X_{c,1}(t)$ and $X_{c,2}(t)$ are indexes of horizontal and vertical location of center of bubble.

The mean velocity of bubble. To observe rising speed of bubble, the following mean velocity of bubble is used.

$$U_c(t) = (U_{c,1}(t), U_{c,2}(t)), \quad U_{c,j}(t) = \frac{1}{|\Omega_2(t)|} \int_{\Omega_2(t)} u_j dx \quad (j = 1, 2). \quad (4.6)$$

$U_{c,2}(t)$ is called *rise velocity*. By the use of $U_{c,1}(t)$, one can investigate horizontal symmetricity of the motion.

Remark 4.1. Since $1 - H(\phi(t))$ is indicator function on $\Omega_2(t)$, $X_{c,j}(t)$ and $U_{c,j}(t)$ ($j = 1, 2$) are computed by the following formulae.

$$\begin{aligned} X_{c,j}(t) &= \int_{\Omega} (1 - H(\phi)) x_j dx \Big/ \int_{\Omega} (1 - H(\phi)) dx, \\ U_{c,j}(t) &= \int_{\Omega} (1 - H(\phi)) u_j dx \Big/ \int_{\Omega} (1 - H(\phi)) dx. \end{aligned}$$

Circularity. The degree of circularity $\chi = \chi(t)$ is defined as

$$\chi(t) = \frac{P_a}{P_b} = \frac{\text{Perimeter of area-equivalent circle}}{\text{Perimeter of bubble}} = \frac{\pi d_a(t)}{P_b}. \quad (4.7)$$

Here $P_a(t)$ denotes the perimeter of a circle with diameter $d_a(t) > 0$ and such a circle has area equal to that of bubble at with perimeter $P_b(t)$.

By the level set function ϕ and approximation of Dirac's delta $\delta_\varepsilon(\phi)$, $P_b(t)$ is given and approximated by

$$P_b(t) = \oint_{\{\phi=0\}} d\sigma \approx \int_{\Omega} \delta_\varepsilon(\phi) dx. \quad (4.8)$$

Additional values. In addition to the above benchmark values, we also observe additional two values for checking SDF property of the level set function ϕ and mass-preservation of fluid 2.

In order to check SDF property of ϕ , we observe L^1 -mean value of $|\nabla\phi|$.

$$\|\nabla\phi(t)\| := \frac{1}{|\Omega|} \int_{\Omega} |\nabla\phi(t, \mathbf{x})| dx. \quad (4.9)$$

If $\phi(t, \mathbf{x})$ satisfies the Eikonal equation $|\nabla\phi(t, \mathbf{x})| = 1$ (a.e.), then $\|\nabla\phi(t)\| = 1$ holds. However, $\|\nabla\phi(t)\| = 1$ does not imply $|\nabla\phi(t, \mathbf{x})| = 1$ (a.e.). Hence, we call $\|\nabla\phi\| = 1$ pseudo SDF property. Since it is hard to check SDF property for every mesh points, we check only pseudo SDF property.

Ideally volume of bubble is preserved. Thus, it is important to check time evolution of volume of bubble in numerical computation. Volume of bubble is Lebesgue measure of $|\Omega_2(t)|$. By using the level set function, $|\Omega_2(t)|$ is given by

$$|\Omega_2(t)| = \int_{\Omega_2(t)} dx = \int_{\Omega} (1 - H(\phi)) dx \approx \int_{\Omega} (1 - H_\varepsilon(\phi)) dx. \quad (4.10)$$

Such a formulation was already used in (4.5) and (4.6).

4.2. Numerical experiments

In this subsection, we shall show our numerical result. The computation was performed on Apple iMac (Late 2012) with 3.4GHz Intel Core i7 processor and 32GB 1600MHz DDR3 memory.

We use FreeFem++¹ [9, 10] for our numerical computation. FreeFem++ is a programming language and software for numerical computation of partial differential equations by means of finite element method. In FreeFem++, there are various linear solvers and various finite elements (for details, see [10]). We solve a linear system derived from (2.21) by UMFPACK, which is a sparse linear solver. We adopted elliptic reinitialization. The maximal observation time is $T_{\max} = 3.0$ and time step size of the following computation is $\tau = 10^{-3}$.

Figure 4.2 shows time evolution of zero level set and velocity vector field of our computation and Figure 4.4 shows trajectory of center of mass $X_c(t_n)$.

We use adaptive mesh refinement (AMR). AMR enables us to capture the interface $\Gamma(t)$ precisely, because we can put much mesh points near the interface. Since we use AMR, number of triangles changes step by step. Average of number of triangles is about 10,000 and number of vertices is about 5,000.

Figure 4.3 shows computational meshes at $t_n = 0.0$ (initial state) and $t_n = 3.0$ (final state). One can see that computational mesh suggests the shape of interface (Fig. 4.3(b) and Fig. 4.2(f)). Such an AMR technique is one of main feature of our computation.

Time sequences of Benchmark values. Figure 4.5 shows time sequences of benchmark values.

Fig 4.5(a), (b) and (c) indicate time sequences of vertical location of center of mass $X_{c,2}(t_n)$, rise velocity $U_{c,2}(t_n)$ and circularity $\chi(t_n)$. Each graph is similar to corresponding one in Hysing *et al.* [11] and Doyeux *et al.* [5]. In particular, our result is similar to that of FreeLIFE (EPFL Lausanne) in [11].

Fig 4.5(d) and (e) indicate time sequences of horizontal location of center of mass $X_{c,1}(t_n)$ and horizontal mean velocity $\overline{U_{c,1}}(t_n)$. These values are used to observation for symmetricity of the rising bubble. $\overline{X_{c,1}} = 0.499992787$ and $\overline{U_{c,1}} = 8.75 \times 10^{-5}$, where $\overline{X_{c,1}}(t_n)$ and $\overline{U_{c,1}}$ denote time average of $X_{c,1}(t_n)$ of $U_{c,1}(t_n)$, respectively. The horizontal motion of bubble is almost symmetric, but from macroscopic view symmetricity of the motion breaks after $t_n > 1$.

Fig 4.5(f) indicates time sequence of $\|\nabla\phi_h(t_n)\|$ from macroscopic view. Time average of $\|\nabla\phi_h\|$ is $\overline{\|\nabla\phi_h\|} = 0.997385$ and the final value is $\|\nabla\phi_h(3.0)\| = 0.993951$. By reinitialization, ϕ_h^n almost satisfies pseudo SDF property for all n .

Fig 4.5(g) indicates time sequence of the volume of fluid 2. Ideally $|\Omega_2(t)|$ must be conserved. However, the final value is $|\Omega_2(3.0)| = 0.193442$. Since $|\Omega_2(0)| = \pi r_0^2 \approx 0.19635$, 1.5% of fluid 2 was lost in our computation.

Acknowledgment. The author would like to express his sincere thanks to Professor Katsuhi Ohmori for fruitful discussion.

References

- [1] C. Basting and D. Kuzmin. A minimization-based finite element formulation for interface-preserving level set reinitialization. *Computing*, 95(1, suppl.):S13–S25, 2013.

¹<http://www.freefem.org/ff++/>

- [2] M. Benítez and A. Bermúdez. A second order characteristics finite element scheme for natural convection problems. *J. Comput. Appl. Math.*, 235(11):3270–3284, 2011.
- [3] S. C. Brenner and L. R. Scott. *The mathematical theory of finite element methods*, volume 15 of *Texts in Applied Mathematics*. Springer, New York, third edition, 2008.
- [4] M. G. Crandall, H. Ishii, and P.-L. Lions. User’s guide to viscosity solutions of second order partial differential equations. *Bull. Amer. Math. Soc. (N.S.)*, 27(1):1–67, 1992.
- [5] V. Doyeux, Y. Guyot, V. Chabannes, C. Prud’homme, and M. Ismail. Simulation of two-fluid flows using a finite element/level set method. Application to bubbles and vesicle dynamics. *J. Comput. Appl. Math.*, 246:251–259, 2013.
- [6] S. Groß, V. Reichelt, and A. Reusken. A finite element based level set method for two-phase incompressible flows. *Comput. Vis. Sci.*, 9(4):239–257, 2006.
- [7] S. Gross and A. Reusken. *Numerical methods for two-phase incompressible flows*, volume 40 of *Springer Series in Computational Mathematics*. Springer-Verlag, Berlin, 2011.
- [8] D. Hartmann, M. Meinke, and W. Schröder. Differential equation based constrained reinitialization for level set methods. *J. Comput. Phys.*, 227(14):6821–6845, 2008.
- [9] F. Hecht. New development in freefem++. *J. Numer. Math.*, 20(3-4):251–265, 2012.
- [10] F. Hecht. *Freefem++*. Laboratoire Jacques-Louis Lions, Université Pierre et Marie Curie, 2015.
- [11] S. Hysing, S. Turek, D. Kuzmin, N. Parolini, E. Burman, S. Ganesan, and L. Tobiska. Quantitative benchmark computations of two-dimensional bubble dynamics. *Internat. J. Numer. Methods Fluids*, 60(11):1259–1288, 2009.
- [12] C. Liu, F. Dong, S. Zhu, D. Kong, and K. Liu. New variational formulations for level set evolution without reinitialization with applications to image segmentation. *J. Math. Imaging Vision*, 41(3):194–209, 2011.
- [13] H. Notsu and M. Tabata. A single-step characteristic-curve finite element scheme of second order in time for the incompressible Navier-Stokes equations. *J. Sci. Comput.*, 38(1):1–14, 2009.
- [14] K. Ohmori and N. Yamaguchi. *in preparation*.
- [15] K. Ohmori and N. Yamaguchi. Visualization of nonlinear phenomena with FreeFem++ and paraview: Application to reaction-diffusion system and fluid dynamics. *Mem. Fac. Human. Devel. Univ. Toyama.*, 9(1):221–241, 2014 (in Japanese).
- [16] K. Ohmori, N. Yamaguchi, N. Hamamuki, and F. Hecht. Numerical investigation of two-fluid flows by FreeFem++ and the mathematical validation of the reinitialization. *in preparation*.
- [17] S. Osher and J. A. Sethian. Fronts propagating with curvature-dependent speed: algorithms based on Hamilton-Jacobi formulations. *J. Comput. Phys.*, 79(1):12–49, 1988.
- [18] O. Pironneau. *Finite element methods for fluids*. John Wiley & Sons Ltd., Chichester, 1989.
- [19] H. Rui and M. Tabata. A second order characteristic finite element scheme for convection-diffusion problems. *Numer. Math.*, 92(1):161–177, 2002.

- [20] J. Shen. On error estimates of the penalty method for unsteady Navier-Stokes equations. *SIAM J. Numer. Anal.*, 32(2):386–403, 1995.
- [21] R. S. Strichartz. *A guide to distribution theory and Fourier transforms*. World Scientific Publishing Co. Inc., River Edge, NJ, 2003.
- [22] M. Sussman and E. Fatemi. An efficient, interface-preserving level set redistancing algorithm and its application to interfacial incompressible fluid flow. *SIAM J. Sci. Comput.*, 20(4):1165–1191 (electronic), 1999.
- [23] M. Sussman, P. Smereka, and S. Osher. A level set approach for computing solutions to incompressible two-phase flow. *J. Comput. Phys.*, 114:146–159, 1994.
- [24] M. Tabata. Finite element schemes based on energy-stable approximation for two-fluid flow problems with surface tension. *Hokkaido Math. J.*, 36(4):875–890, 2007.
- [25] R. Temam. Une méthode d’approximation de la solution des équations de Navier-Stokes. *Bull. Soc. Math. France*, 96:115–152, 1968.
- [26] A.-K. Tornberg and B. Engquist. A finite element based level-set method for multiphase flow applications. *Comput. Vis. Sci.*, 3(1-2):93–101, 2000.
- [27] N. Yamaguchi. Mathematical justification of the penalty method for viscous incompressible fluid flows. *RIMS Kōkyūroku*, 1830:127–142, 2013.

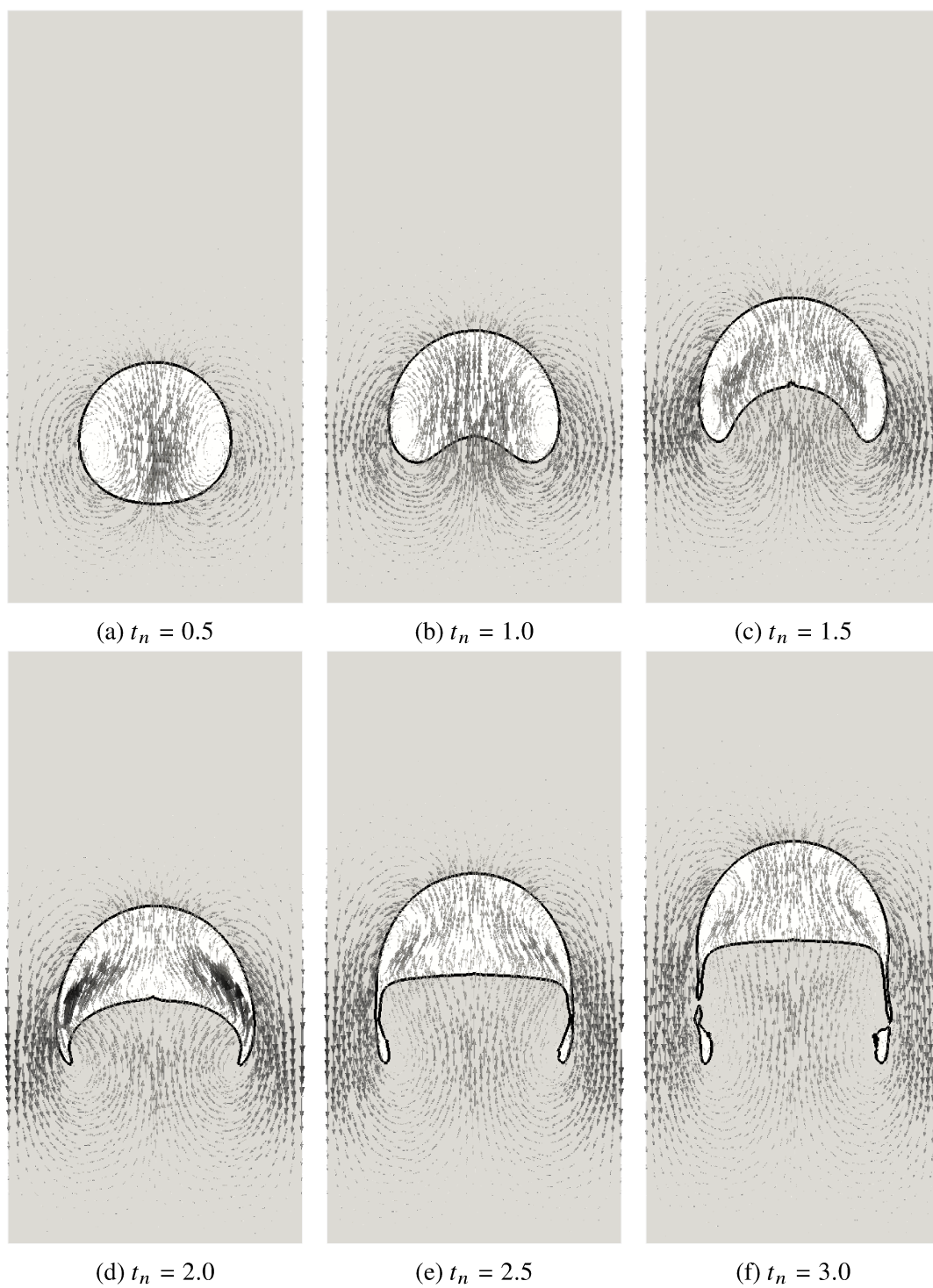


Figure 4.2: Time evolution of the zero level set of $\phi_h(t_n)$ and velocity vector fields. Solid black line indicates the zero level set of $\phi_h(t_n)$.

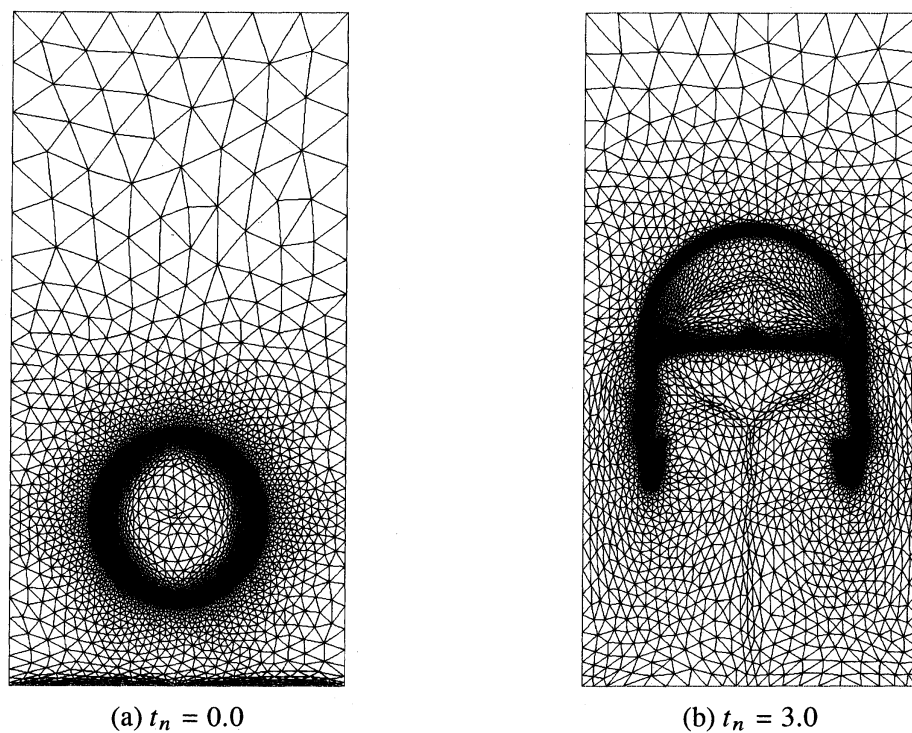


Figure 4.3: Computational meshes

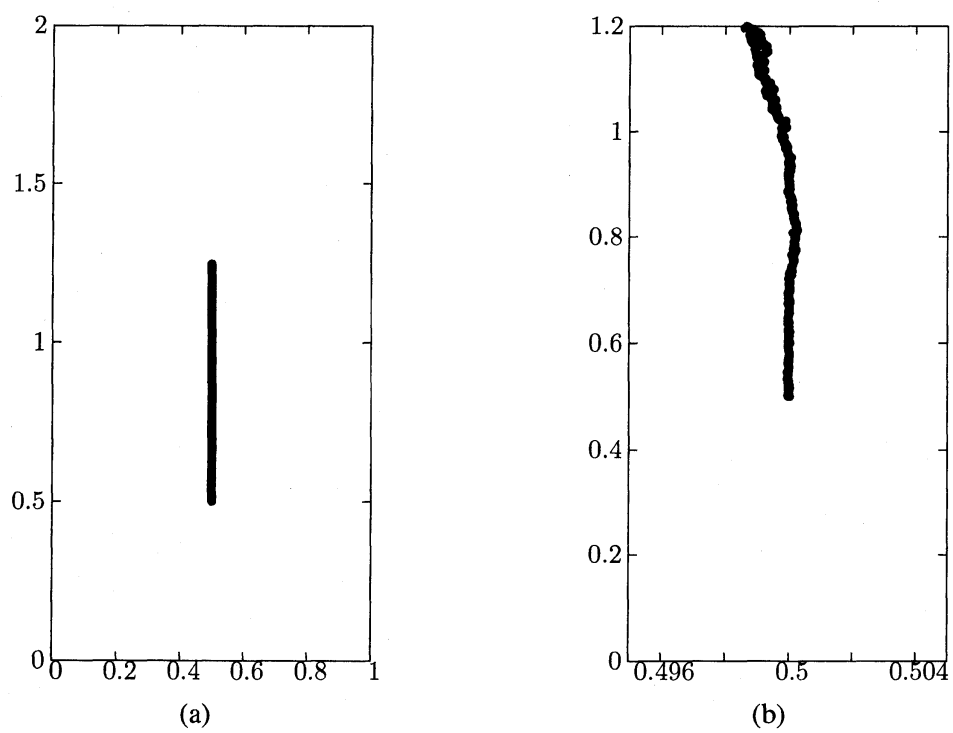


Figure 4.4: Trajectory of center of mass

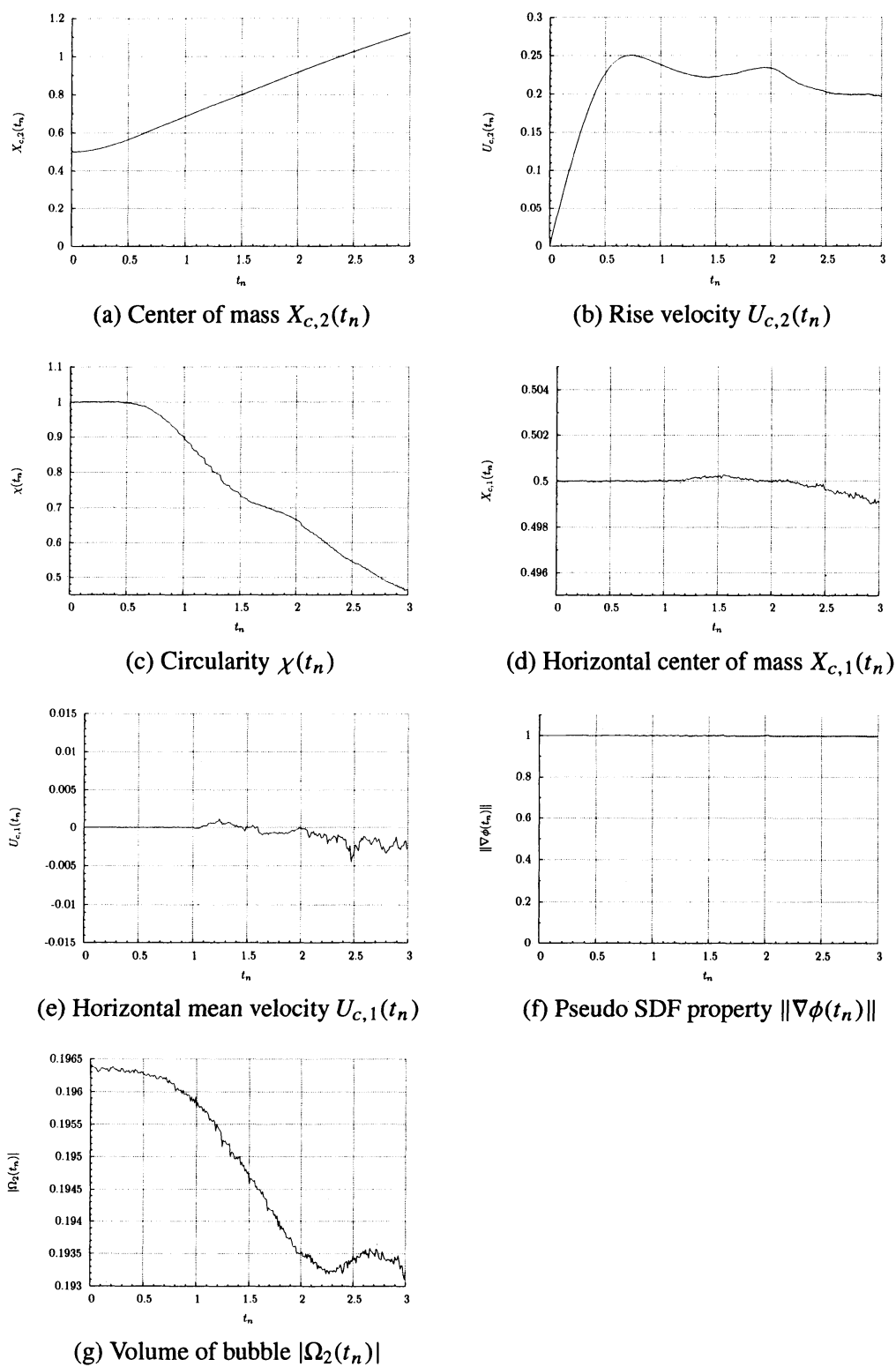


Figure 4.5: Time sequences of benchmark values